Molecular Dynamics Simulations of Water Transport through Butanol Films

A. Gilde, N. Siladke, and C. P. Lawrence*

Department of Chemistry, Grand Valley State University, Allendale, Michigan 49401

Received: March 24, 2009; Revised Manuscript Received: May 08, 2009

It is well-known that well-formed monolayers of long-chain alcohols on water dramatically reduce the rate of water evaporation. Recent experiments, however, have shown that the short-chain surfactant butanol has a negligible effect on the rate of water evaporation from a solution of supercooled sulfuric acid. We used molecular dynamics simulations to examine the condensation of water through a layer of butanol coating water. From those simulations, we observed a reduction in the rate of water condensation by a factor of 3 which would imply a similar reduction in the rate of evaporation. It was observed that a vapor molecule would condense only if it formed a long-lived hydrogen bond with another molecule and that there was no dependence on the initial velocity of the vapor molecule. The ability of the surfactant to participate in hydrogen bonding was found to facilitate the condensation of water into the bulk.

1. Introduction

Tropospheric aerosols play a tremendous role in the planet's climate through processes such as cloud formation and radiation reflection.[1−7] They also provide a medium upon which reactions may occur.[8,9] All of these functions are impacted by their growth and dissipation through condensation and evaporation. It has recently been discovered that these aerosols contain substantial amounts of organic material that may coat the surface of the aerosol.[10−13] The role that these surfactant molecules play in the processes discussed above is not well understood.

A monolayer of hexadecanol on a water surface slows the rate of water evaporation by 4 orders of magnitude. Experiments indicate a roughly exponential dependence on the chain length for alcohols ranging from 14 to 22 carbon atoms.[14,15] If one were to extrapolate this trend to butanol, it would be expected that the rate of evaporation would drop by a factor of 5 from pure water. Such an extrapolation is questionable as the observed impedance to the transport of water molecules is understood to be caused by the tight packing of the carbon chains in the long-chain surfactants. However, in the case of butanol, the carbon chains do not attract each other nearly as strongly, leading the surface to be much more disordered.[16] This disorder might allow for gaps in the surfactant layer that escaping water molecules could slip through, and thus greatly reduce the influence of the surfactant. Nathanson et al. observed that when butanol coats a layer of supercooled sulfuric acid, there is no measurable difference in the rate of water evaporation compared to evaporation from the bare acid.[17] Even more surprising is the observation that the butanol layer actually leads to an increase in the uptake of HCl and HBr into the bulk sulfuric acid.[18,19]

In this article, molecular dynamics simulations were used to explore the process by which water condenses through a short-chain alcohol surfactant coating room temperature water. We examined condensation, rather than the analogous process of evaporation, because evaporation events occur rather infrequently on the time scale of the simulation. Condensation, however, can be initiated by inserting a water molecule in the gas phase and allowing it to collide with the interface.[20] This process can be repeated with a relatively high frequency to expedite data collection. The result is a measure of the fraction of colliding molecules that successfully condense into the liquid or the condensation coefficient. The rate of condensation is then calculated via

$$\text{rate} = \alpha x \tag{1}$$

where α is the condensation coefficient and x is the rate at which vapor molecules collide with the surface, which is determined using statistical mechanics. Since the rates of evaporation and condensation are equal at equilibrium, this approach gives the evaporation rate.

Previous simulation work found a condensation coefficient of about unity for water condensing onto pure water.[20−22] Experimental measures of this quantity vary widely, ranging from 0.1 to 1.[23−32] However, the most recent and comprehensive experiments found a value of 0.2 ± 0.1.[32] The classical simulations that are used to probe these interactions are by no means perfect. In particular, the SPC/E model[33] (which is used here) is known to underestimate the vapor pressure and the surface tension and overestimate the bulk density.[34−36] Despite these flaws, these simulations can provide valuable insight regarding the transport of water through a surfactant at the molecular level that is not accessible experimentally.

2. Simulation Methods

The classical molecular dynamics simulations were performed using the SPC/E model for water[33] and the TraPPE-UA force field (a unified atom model) for the alcohols.[37] In addition to the intermolecular interactions described by the SPC/E model, harmonic force constants were employed for internal motion.[38] Rectangular periodic boundary conditions were applied, and the electrostatic forces were calculated using the damped shifted force alternative to the Ewald summation as described by Fennell and Gezelter.[39−41] The damping parameter, α, was 0.2 $Å^{-1}$, and the cutoff radius was set to 12.3 Å (half of the shortest of the box lengths). The equations of motion were integrated using the leapfrog algorithm with a time step of 0.5 fs. In all cases, the temperature was held constant through velocity scaling

* To whom correspondence should be addressed. E-mail: lawrechi@gvsu.edu.

10.1021/jp9026699 CCC: $40.75
Published on Web 07/01/2009

at each step. Initially, a cubic system containing 500 water molecules was prepared in which the box length was chosen such that the density of the system would be equal to the experimental value at 300 K. Velocities were randomly assigned to each atom. The system was equilibrated for 250 ps.

To prepare a water interface, the length of the box was extended in one dimension (z) to 100 Å (about four times the length in the original cubic box). To allow the system to re-equilibrate after this change, an additional run of 250 ps was performed. For the water/surfactant systems, when the original cubic box was extended, a layer of evenly spaced alcohol molecules was added to the upper and lower interfaces followed by an equilibration run of 250 ps. Simulations were run with surfactant coverages of 0.7, 1.5, 2.6, 4.1, 5.9, and 8.1 molecules/nm^2.

After the interfaces were prepared, the scattering simulations were performed by introducing water molecules in the vapor region of the system. The velocities of these molecules were selected on the basis of the Boltzmann distribution for the translational, rotational, and vibrational degrees of freedom. The bonds were also randomly displaced from equilibrium in the same manner.[42] Each molecule was randomly placed in the x- and y-dimensions and positioned about 10 Å from the interface along the z-axis. When the velocity in that direction was assigned to be positive, the molecule approached the lower interface, and when the z velocity was negative, the molecule approached the upper interface. Once this molecule had collided with another (defined by an oxygen−oxygen or oxygen−carbon distance of less than 4 Å), the simulation continued for an additional 10 ps. At this point, we would return to the original equilibrated interface and insert another vapor molecule. For each system, 250 scattering trajectories were calculated.

3. Results and Discussion

To characterize the interfaces, we first examined the longitudinal density profiles of the water and the surfactant. For this calculation, we divided the system into 100 slices, each with a thickness of 1 Å. Running the simulation over a period of 500 ps, we determined the average number of molecules in each of those slices. As the mass of the water molecules is almost entirely on the oxygen atom, we tracked these molecules as a single entity on the basis of the position of that atom. For the surfactant molecules, this assignment was less clear as it would be perfectly reasonable for the molecule to span several different slices. We tracked several different atoms independently: the H and O from the alcohol group, the α-methylene group, and the methyl tail. Examples of these density profiles are shown in Figure 1.

The thickness of the interface was found by fitting the density profile for the water molecules to

$$\rho(z) = \frac{1}{2}(\rho_L + \rho_V) - \frac{1}{2}(\rho_L - \rho_V)\tanh\left(2.1972\frac{z - z_0}{t}\right) \quad (2)$$

where ρ_L and ρ_V are the densities of the liquid and vapor, respectively, z_0 is the location of the Gibbs dividing surface (the point at which the density is the average of ρ_L and ρ_V), and t is the 90−10 interface thickness which is defined as the distance over which the density falls from 90% of the bulk value to 10% of the bulk value.[43,44] The density profile of the water molecules was fit to this expression, and the value of t is given in Table 1 as a function of butanol coverage.

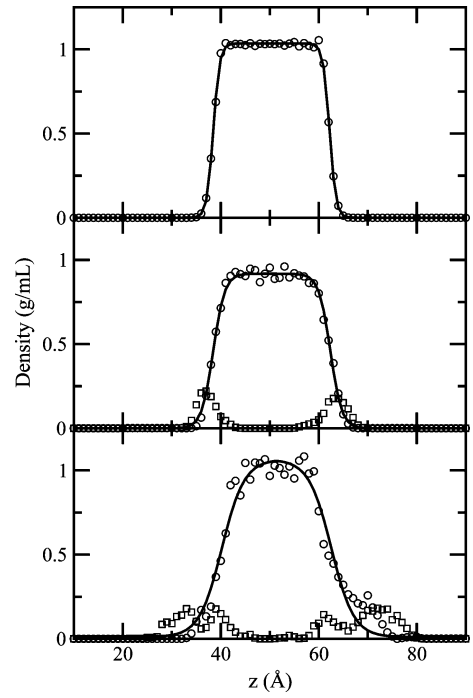

Figure 1. Longitudinal density profiles for three different systems. The top, middle, and bottom panels refer to pure water, water coated with 4.1 butanol molecules/nm^2, and water coated with 8.1 butanol molecules/nm^2, respectively. The circles are the values calculated at each position for the water molecules, and the squares represent the oxygen atoms of the butanol molecules. The water data has been fit to eq 2, and the results are shown as the solid lines.

TABLE 1: 90−10 Interface Thickness, t, for Various Butanol Coverages

coverage (molecules/nm^2)	t (Å)
0	2.86
4.1	5.13
8.1	10.06

To better understand how a water molecule can escape from or pass through the surfactant layer, we also examined the way in which the surfactant molecules were oriented. In Figure 2, we show the distribution of heights of the butanol molecules as a function of surface coverage. For the upper interface, the height of the molecule was defined as the difference in the z-coordinate between the methyl groups at its tail and the H atom at the head of the molecule, $z_C - z_H$. If the molecules were uniformly standing upright, we would expect the distribu-

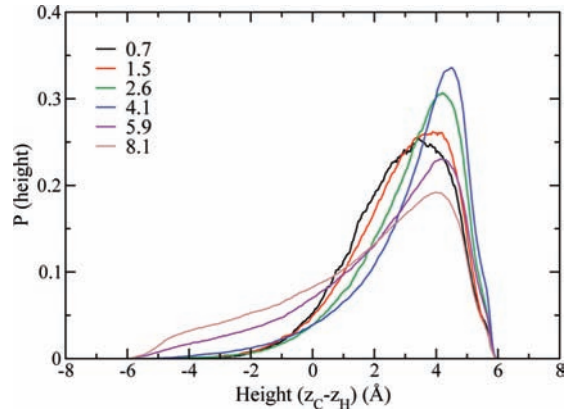

Figure 2. Distribution of heights of the butanol molecules. The curves are labeled by the number of butanol molecules/nm^2.

TABLE 2: Average Height of the Butanol Molecules as Surface Coverage Is Varied

coverage (molecules/nm^2)	average height (Å)
0.7	2.8
1.5	2.9
2.6	3.2
4.1	3.3
5.9	2.3
8.1	1.7

tion to be sharply peaked at about 6 Å. Conversely, if the molecules had a tendency to lie flat on the surface of the liquid, the distribution would be peaked near zero. We included the lower interface in this calculation by defining the height as $z_H - z_C$. By doing so, we obtain a positive value for the height when the methyl tail is dangling away from the interface. As shown in this figure, the distribution becomes sharper as surface coverage increases until it reaches a maximum at 4.1 butanol molecules/nm^2. For greater coverage, the distribution becomes much broader as there is a pronounced tendency for the butanol molecules to begin forming a bilayer. The formation of the bilayer is apparent in Figure 2 as negative heights; the molecules have changed directions so that the polar head of the molecule is directed toward the vapor. To quantify this trend, the average height is given in Table 2.

When a water molecule scatters from the surface of the water, the trajectory was divided into three classes. Intuitively, we would have two categories: inelastic scattering and condensation. The trajectory was labeled as scattering when the incoming water molecule struck the surface and bounced directly off. A condensation was deemed to occur when the water molecule collided with the surface and remained at the surface or within the bulk throughout the entire time the molecule was observed (10 ps). A third category (desorption) was needed as we observed some molecules that would hit the surface, remain in contact for some period of time, and then drift away. It was typically the case that condensing molecules would penetrate significantly deeper into the bulk than those that were observed to drift away. Examples of these three types of trajectory are shown in Figure 3. While these three sample trajectories approach the surface with very different velocities due to random sampling from the Boltzmann distribution, no correlation was found between the incident velocity and the fate of the molecule.

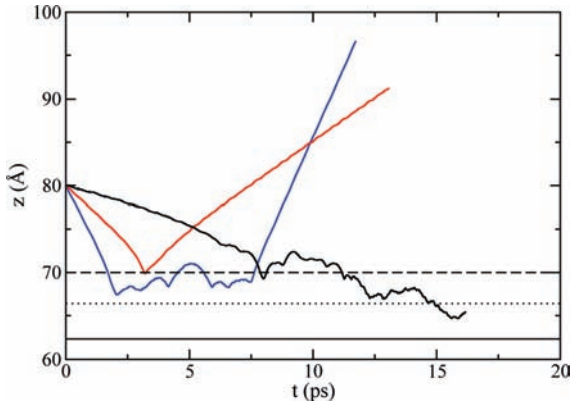

Figure 3. Sample trajectories showing the paths a colliding molecule may take. The black curve is a condensation, the red curve is a scatter, and the blue curve is a desorption. The solid, dotted, and dashed lines represent the position of the water, the oxygen of the butanols, and the carbon tail of the butanols, respectively. In all three cases, the position is identified as the point at which the density of the molecules (atoms) is the average of the maximum and minimum values.

TABLE 3: Percentage of Trajectories that Condense, Scatter, and Desorb from the Surface

coverage (molecules/nm^2)	condense	scatter	desorb
0.0	100	0	0
0.7	91	2	7
1.5	83	6	11
2.6	60	24	16
4.1	33	38	28
5.9	37	43	20
8.1	52	31	17

In examining these trajectories further, we tracked the hydrogen bonds that the incoming water molecule formed. A hydrogen bond was defined as having an oxygen−oxygen distance and an oxygen−hydrogen distance less than their respective minima in their pair-correlation functions. While it is more common that an angular criterion is used in place of the oxygen−hydrogen distance, they do serve the same purpose: restricting hydrogen bonds to be relatively linear.[45−47] Only those trajectories that resulted in condensation were found to form long-lived hydrogen bonds. In the other two cases, the majority of the trajectories displayed no hydrogen bonding at all, although occasionally a hydrogen bond would form for a very brief time (on the order of 100 fs). It should be noted that, while hydrogen bonding correlated strongly with whether a trajectory resulted in condensation, it was not used to make this classification. The percentages of trajectories for the three different categories are shown in Table 3, and the condensation coefficient (fraction of trajectories that successfully condense) is plotted versus surface coverage in Figure 4.

The first concern was whether the 10 ps of observation after colliding with the surface was sufficient. To confirm that this was acceptable, the trajectories for a coverage of 4.1 butanol molecules/nm^2 were calculated for 150 ps after the initial collision. Of the 89 trajectories that were initially classified as condensations, only six left the bulk in the time observed. Four of those six trajectories never formed a hydrogen bond during their contact with the surface and the two that did formed them only very briefly while the reminaing 83 trajectories displayed long-lived hydrogen bonding between the incoming water molecule and those in the bulk. This provides further evidence for the correlation between the formation of hydrogen bonds during the initial interaction with the surface and condensation. Previous researchers have made the distinction between absorption (the incoming molecule enters the bulk) and adsorption (the incoming molecule remains in the interfacial region).[48] During the original run in which the trajectories were only calculated for 10 ps, only a fifth of those deemed to condense

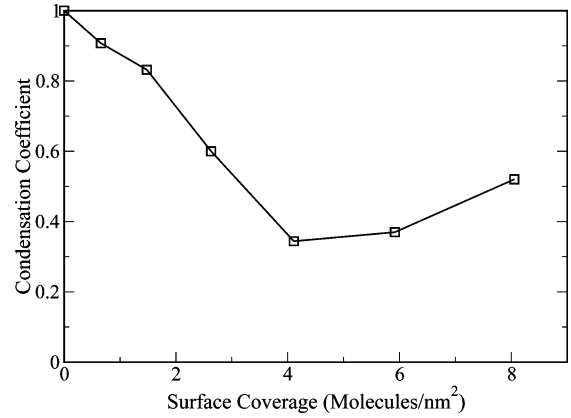

Figure 4. Condensation coefficient as a function of butanol coverage.

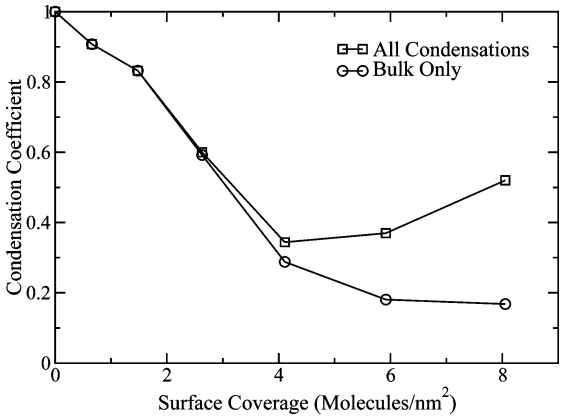

Figure 5. Condensation coefficient as a function of butanol coverage using two different definitions of condensation.

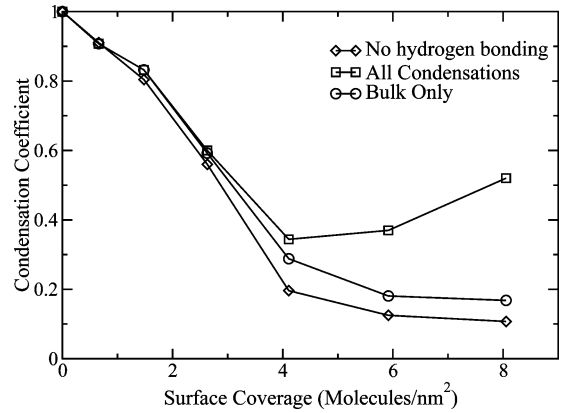

Figure 6. Condensation coefficient as a function of butanol coverage with no hydrogen bonding between the incoming water molecule and the surfactant.

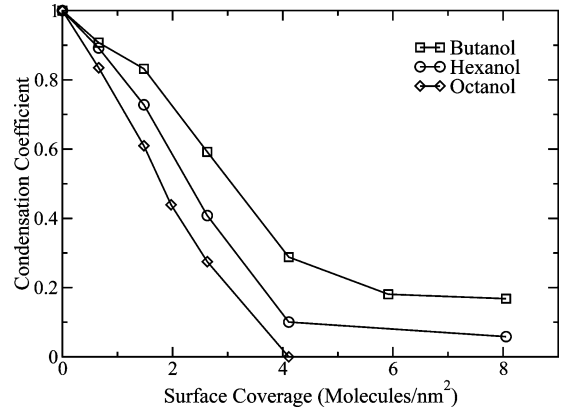

Figure 7. Condensation coefficient as a function of surfactant coverage using three different alcohols.

entered the bulk of the water layer. However, in this longer run, all of those that condensed successfully reached the bulk.

Convinced that our observation time was sufficient, our attention was then drawn to the rise in the condensation coefficient at high surface coverage. At high coverage, while a greater portion of the molecules was condensing using the definition posed above, relatively few of these molecules formed hydrogen bonds with other water molecules; most formed them with the surfactant. At these very high levels of coverage, the butanol surfactant begins to separate into a bilayer. This separation increases the exposure of the OH groups of some of these surfactant molecules to the vapor, resulting in an increase in the condensation coefficient of water. This led us to consider an alternate tracking of condensation in which only those molecules that actually made contact with other water molecules are counted. With this modification, we find the more intuitive result that increasing the surfactant coverage leads to a monotonic decrease in the ability of the incoming water molecules to penetrate that layer as shown in Figure 5. This led us to question the ultimate fate of these molecules. When the trajectories for a coverage of 8.1 molecules/nm^2 were examined for longer periods of time (150 ps) after their initial interaction with the surface, it was found that they never did escape back into the vapor, but very few of them (less than 3%) were incorporated into the bulk.

To further explore the mechanism of penetration through this layer, we repeated these simulations with the provision that the incoming water molecule had no electrostatic interaction with the surfactant. However, this interaction was maintained between the surfactant and the bulk water. This effectively turns off the possibility of hydrogen bonding between the condensing water and the butanol molecules, but does not alter the structure of the surface. The results of these simulations are shown in Figure 6. The primary effect here is that the condensation coefficient no longer rises at high concentration as the molecules that were previously trapped by the surfactant will scatter. There is a large drop in the condensation coefficient at all levels of coverage (nearly a factor of 2 at 4.1 butanol molecules/nm^2), indicating that the ability to hydrogen bond to the surfactant plays a role in condensation even when the surfactant exists as a well-defined monolayer. This has been observed experimentally in that a hydrogen-bonding surfactant enhances the uptake of acids (HCl and HBr) into supercooled sulfuric acid.[18,19]

Using the extrapolation of the experimental data on the effect of long-chain alcohols, we predicted that if the butanol molecules were replaced with hexanol, we would see a further reduction in the condensation coefficient of about 2.3 for a complete monolayer (with a coverage between 4.2 and 5.0 molecules/nm^2).[14,15] Using the same models,[33,37] we repeated our calculations with hexanol as the surfactant. These data are shown in Figure 7. Using the data at 4.1 molecules/nm^2 which correspond to the tightest surfactant layer in the butanol, we found a reduction of about 2.9. The trend continues when octanol is used as the surfactant, but the condensation coefficient was sufficiently small at 4.1 molecules/nm^2 that we were unable to determine that value with a high enough precision to comment on it quantitatively. As noted in the Introduction, such an extrapolation is not expected to be very reliable, but it does bolster the argument that our simulations qualitatively capture the experimentally observed phenomena.

4. Conclusions

At low butanol coverage, the surfactant molecules are fairly disordered. As the level of coverage increases, the surfactant layer becomes tighter and the molecules begin to align vertically. The tightest layer observed is at 4.1 molecules/nm^2. When we attempt to add additional surfactant molecules, they tend to split into two separate layers.

Unless the incoming vapor molecule forms a hydrogen bond when it collides with the surface, it will fail to condense. The condensation coefficient falls as the layer becomes tighter and then rises again when the butanol bilayer begins to form. When there is a bilayer of surfactant, the OH groups of these molecules become exposed to the incoming water molecule, allowing it to form its hydrogen bond with the butanol instead of the bulk water. If we instead only counted those vapor molecules that

formed hydrogen bonds to other water molecules as having condensed, we find the anticipated result that the condensation coefficient monotonically decreases as the coverage increases. However, nearly all of the condensing water molecules remain in the interfacial region for extended periods of time. This method of counting gives very similar results to running the simulation having turned off the electrostatic (hydrogen bonding) interactions between the incoming vapor molecule and the surfactant.

Our simulations indicate that the presence of a butanol monolayer leads to a reduction of the rate of water evaporation by a factor of about 3. This result differs from the experiments of Nathanson et al., who observed that a similar coverage of butanol has almost no effect on the rate of evaporation.[17] However, those experiments were performed with supercooled sulfuric acid instead of room temperature water. We anticipate that the difference in the nature of the bulk will account for much of the difference between the computed and experimental evaporation rates. It would appear that the temperature of the vapor molecule would not be relevant as the velocity of the incoming vapor molecule had no observed effect on the fate of that molecule. However, the lower temperature will alter the nature of the surface substantially. The presence of ions at the surface could also increase the driving force for condensation. Despite the deviation between the experimental observations of Nathanson et al. and our simulations, extrapolating experimental data for long-chain alcohols on water leads one to predict a reduction in the condensation coefficient by a factor of about 5,[14,15] much closer to our observations. Our result also stands in contrast of Morita's simulations of the condensation of methanol into mixtures of methanol and water, in which he found that the condensation coefficient remained near unity independent of the composition of the bulk.[49] The implication of his study would be that the hydrophobicity of the surface does not hinder condensation. Examination of the trajectories that resulted in inelastic scattering indicates that many of these waters are deflected from the surface by the butanol tail. As this is quite unlikely to occur with a methanol surfactant, it is no suprise then that the condensation coefficient would be much higher in Morita's system.

Acknowledgment. We thank J. R. Schmidt and Gilbert Nathanson for helpful discussions. We are grateful for generous support from the Petroleum Research Fund through Grant PRF# 44874-GB 6 and the Michigan Space Grant Consortium.

References and Notes

(1) Chuang, P. Y.; Charlson, R. J.; Seinfeld, J. H. *Nature* **1997**, *390*, 594.
(2) Hudson, J. G.; Yum, S. S. *J. Geophys. Res.* **1997**, *54*, 2642.
(3) Yum, S. S.; Hudson, J. G.; Xie, Y. *J. Geophys. Res.* **1998**, *103*, 16625.
(4) Nenes, A.; Ghan, S.; Abdul-Razak, H.; Chuang, P. Y.; Seinfeld, J. H. *Tellus, Ser. B* **2001**, *53*, 133.
(5) Charlson, R. J.; Schwartz, S. E.; Hales, J. M.; Cess, R. D.; Coakley, J. A., Jr.; Hansen, J. E.; Hofmann, D. J. *Science* **1992**, *255*, 423.
(6) Houghton, J. T. *Climate Change 2001: The Scientific Basis*; Cambridge University Press: Cambridge, UK, 2001.
(7) Rosenfeld, D. *Science* **2000**, *287*, 1793.
(8) Hanson, D. R. *J. Phys. Chem. B* **1997**, *101*, 4998.
(9) Worsnop, D. R.; Morris, J. W.; Shi, Q.; Davidovits, P.; Kolb, C. E. *Geophys. Res. Lett.* **2002**, *29*, 1996.
(10) Murphy, D. M.; Thomson, D. S.; Mahoney, T. M. *Science* **1998**, *282*, 1664.
(11) Russell, L. M.; Maria, S. F.; Myneni, S. C. B. *Geophys. Res. Lett.* **2002**, *29*, 1779.
(12) Tervahattu, H.; Juhanoja, J.; Kupiainen, K. *J. Geophys. Res. Atmos.* **2002**, *107*, 4319.
(13) Tervahattu, H.; Juhanoja, J.; Vaida, V.; Tuck, A. F.; Niemi, J. V.; Kupiainen, K.; Kulmala, M.; Vehkamaki, H. *J. Geophys. Res. Atmos.* **2005**, *110*, D06207.
(14) Mer, V. K. L.; Healty, T. W.; Aylmore, L. A. G. *J. Colloid Sci.* **1964**, *19*, 673.
(15) Barnes, G. T. *Colloids Surf., A* **1997**, *126*, 149.
(16) Van Loon, L. L.; Minor, R. N.; Allen, H. C. *J. Phys. Chem. A* **2007**, *111*, 7338.
(17) Lawrence, J. R.; Glass, S. V.; Nathanson, G. M. *J. Phys. Chem. A* **2005**, *109*, 7449.
(18) Lawrence, J. R.; Glass, S. V.; Park, S.-C.; Nathanson, G. M. *J. Phys. Chem. A* **2005**, *109*, 7458.
(19) Glass, S. V.; Park, S.-C.; Nathanson, G. M. *J. Phys. Chem. A* **2006**, *110*, 7593.
(20) Morita, A.; Sugiyama, M.; Kameda, H.; Koda, S.; Hanson, D. R. *J. Phys. Chem. B* **2004**, *108*, 9111.
(21) Matsumoto, M. *Fluid Phase Equilib.* **1995**, *144*, 307.
(22) Tsuruta, T.; Nagayama, G. *J. Phys. Chem. B* **2004**, *108*, 1736.
(23) Mills, A. F.; Seban, R. A. *Int. J. Heat Mass Transfer* **1967**, *40*, 2963.
(24) Maa, J. R. *Ind. Eng. Chem. Fundam.* **1969**, *8*, 564.
(25) Wenzel, H. *Int. J. Heat Mass Transfer* **1969**, *12*, 125.
(26) Bonacci, J. C.; Myers, A. L.; Nongbri, G.; Eagleton, L. C. *Chem. Eng. Sci.* **1976**, *31*, 609.
(27) Hatamiya, S.; Tanaka, H. *Proc. Int. Heat Transfer Conf., 8th* **1986**, *4*, 1671.
(28) Fujikawa, S.; Maerefat, M. *Trans. Jpn. Soc. Mech. Eng., B* **1990**, *56*, 1376.
(29) Maerefat, M.; Akamatsu, T.; Fujikawa, S. *Exp. Fluids* **1990**, *9*, 345.
(30) Tsuruta, T.; Masuoka, T.; Kato, Y. *Therm. Sci. Eng.* **1994**, *2*, 98.
(31) Shaw, R. A.; Lamb, D. *J. Chem. Phys.* **1999**, *111*, 10659.
(32) Li, Y. Q.; Davidovits, P.; Shi, Q.; Jayne, J. T.; Kolb, C. E.; Worsnop, D. R. *J. Phys. Chem. A* **2001**, *105*, 10627.
(33) Berendsen, H. J. C.; Grigera, J. R.; Straatsma, T. P. *J. Phys. Chem.* **1987**, *91*, 6269.
(34) Taylor, R. S.; Dang, L. X.; Garrett, B. C. *J. Phys. Chem.* **1996**, *100*, 11720.
(35) Chen, B.; Xing, J.; Siepmann, J. I. *J. Phys. Chem. B* **2000**, *104*, 2391.
(36) Vega, C.; de Miguel, E. *J. Chem. Phys.* **2007**, *126*, 154707.
(37) Chen, B.; Potoff, J. J.; Siepmann, J. I. *J. Phys. Chem. B* **2001**, *105*, 3093.
(38) Toukan, K.; Rahman, A. *Phys. Rev. B* **1985**, *31*, 2643.
(39) Fennell, C. J.; Gezelter, J. D. *J. Chem. Phys.* **2006**, *124*, 234104.
(40) Wolf, D.; Keblinski, P.; Phillpot, S. R.; Eggebrecht, J. *J. Chem. Phys.* **1999**, *110*, 8254.
(41) Zahn, D.; Schilling, B.; Kast, S. M. *J. Phys. Chem. B* **2002**, *106*, 10725.
(42) McQuarrie, D. A. *Statistical Mechanics*; Harper and Row: New York, 1976.
(43) Townsend, R. M.; Gryko, J.; Rice, S. A. *J. Chem. Phys.* **1985**, *82*, 4391.
(44) Matsumoto, M.; Kataoka, Y. *J. Chem. Phys.* **1988**, *88*, 3233.
(45) Bertolini, D.; Cassettari, M.; Ferrario, M.; Grigolini, P.; Salvetti, G. *Adv. Chem. Phys.* **1985**, *62*, 277.
(46) Luzar, A.; Chandler, D. *Phys. Rev. Lett.* **1996**, *76*, 928.
(47) Martí, J. *J. Chem. Phys.* **1999**, *110*, 6876.
(48) Vieceli, J.; Roeselova, M.; Potter, N.; Dange, L. X.; Garrett, B. C.; Tobias, D. J. *J. Phys. Chem. B* **2005**, *109*, 15876.
(49) Morita, A. *Chem. Phys. Lett.* **2003**, *375*, 1.

JP9026699